5-12-2004

Synthetic Defocus for Interferometric Lithography

Frank C. Cropanese
Rochester Institute of Technology

Anatoly Bourov
Rochester Institute of Technology

Yongfa Fan
Rochester Institute of Technology

Jianming Zhou
Rochester Institute of Technology

Lena Zayalova
Rochester Institute of Technology

See next page for additional authors

Recommended Citation

Frank C. Cropanese, Anatoly Bourov, Yongfa Fan, Jianming Zhou, Lena Zavyalova, Bruce W. Smith, "Synthetic defocus in interferometric lithography", Proc. SPIE 5754, Optical Microlithography XVIII, (12 May 2004); doi: 10.1117/12.602948; https://doi.org/10.1117/12.602948

Synthetic defocus for interferometric lithography

Frank C. Cropanese*, Anatoly Bourov, Yongfa Fan, Jianming Zhou, Lena Zavyalova, and Bruce W. Smith
Center for Nanolithography Research, Rochester Institute of Technology
82 Lomb Memorial Drive, Rochester, NY, USA 14623

ABSTRACT

Interference lithography has been widely utilized as a tool for the evaluation of photoresist materials, as well as emerging resolution enhancement techniques such as immersion lithography. The interferometric approach is both simple and inexpensive to implement, however it is limited in its ability to examine the impact of defocus due to the inherently large DOF (Depth-of-Focus) in two-beam interference. Alternatively, the demodulation of the aerial image that occurs as a result of defocus in a projection system may be synthesized using a two pass exposure with the interferometric method. The simulated aerial image modulation for defocused projection systems has been used to calculate the single beam exposure required to reproduce the same level of modulation in an interferometric system through the use of a "Modulation Transfer Curve". The two methods have been theoretically correlated, by way of modulation for projection illumination configurations, including quadrupole and annular. An interferometric exposure system was used to experimentally synthesize defocus for modulations of 0.3, 0.5, 0.7 and 1.0. Feature sizes of 90nm were evaluated across dose and synthetic focus.

Keywords: Interference, interferometric lithography, synthesis, single beam attenuation, defocus, contrast

1. INTRODUCTION

The demand for faster microprocessors, minimal device footprints, and the desire to sustain Moore's law for years to come has stressed the need for novel techniques to achieve increasingly smaller critical dimensions (CD's). The utilization of resolution enhancement technology (RET), such as high NA, phase-shift masking and partially coherent illumination, has supplied the means to preserve optics as the mainstay of modern microlithography. In order to facilitate the continued use of optical methods, innovative approaches must be developed that may be researched and enhanced reliably and with a considerable degree of cost efficiency. Interferometric lithography has been of substantial use in providing a way to examine these approaches.

Interferometric lithography (IL) is based on the interference of two mutually coherent light beams of wavelength λ at the surface of a photosensitive substrate. The interfering beams produce a high contrast sinusoidal intensity pattern that exposes a periodic array of lines and spaces in the photosensitive material. The contrast of these patterns is maintained over a large depth of focus on the order of centimeters, which may be considered infinite. The depth of focus is limited by unmatched path lengths in each arm of the interferometer that are induced by variations in the beam diameter, beam intensity profile and the angle of intersection.[1] The minimum resolvable linewidth in an IL system decreases as the angle of incidence increases. Therefore, the minimum period that may be achieved is $\lambda/2n$, which allows for resolution far exceeding a quarter-wavelength when an immersion medium is introduced. This is possible since interferometric lithography may be described as having a k_1 of 0.25. Simple adjustments may be made to the angle of interference that will allow a wide range of pitches to be studied.

Significant control over aerial image modulation is also possible by unbalancing the intensities of the interferometer arms. Attenuation of one of the two interfering beams in an interferometric lithography system enables the synthesis of attributes of projection lithography, such as defocus,. The intensity imbalance causes only a portion of the unattenuated beam to interfere with the other, leaving behind excess illumination that resembles the intensity bias typically attributed to the 0^{th} diffraction order. This intensity bias can be utilized to induce demodulation in the resulting intensity profile of the interfering beams, which can be correlated to a similar demodulation effect that occurs when defocus is introduced to a projection lithography system.

*fcc8004@cis.rit.edu

Optical Microlithography XVIII, edited by Bruce W. Smith,
Proceedings of SPIE Vol. 5754 (SPIE, Bellingham, WA, 2005)
0277-786X/05/$15 · doi: 10.1117/12.602948

2. MODULATION IN TWO-BEAM INTERFERENCE

The Principle of Superposition is utilized to derive the intensity distribution resulting from the interference of two beams of light. The electric field distribution $\vec{E}$ at a point in space is found by summing the component electric fields of each source and then taking the squared magnitude to obtain the intensity. The expression for the resulting intensity from two-beam interference, assuming levels of modulation less than unity by including a modulation factor *m*, is:

$$I = \frac{1}{2} + \frac{1}{2} m \cos\delta \tag{1}$$

The maximum intensity in equation (1) has been normalized and *m* is restricted to values greater than or equal to zero, and less than or equal to one. The modulation term *m* arises from a number of factors including illumination coherence and polarization. Imbalanced intensities between the two interfering beams also contribute to the level of modulation. The modulation term may be broken down into the product of the individual contributions such that:

$$\begin{aligned} m &= \left|\gamma_{12}\right| a_P a_I \\ I &= \frac{1}{2} + \frac{1}{2}\left|\gamma_{12}\right| a_P a_I \cos\delta \end{aligned} \tag{2}$$

where $\left|\gamma_{12}\right|$ is the contribution due to coherence, a_P is the polarization contribution and a_I is the modulation due to intensity imbalance. An examination of Figure 1 is helpful when deriving the impact of polarization on the modulation of the two-beam interference intensity pattern. When considering polarization, the electric field vectors may be broken down into their TE and TM polarization components, as pictured:

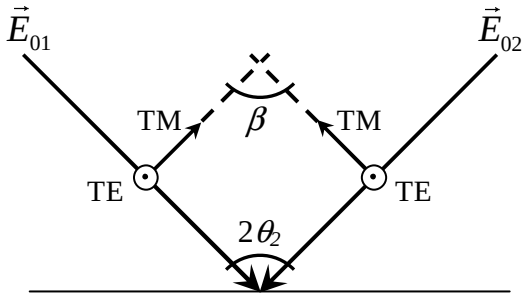

Figure 1. Two-beam interference with each interfering beam broken down into its TE and TM components.

Regardless of the angle of interference $2\theta_2$, the TE components (polarization out of the page) of the interfering beams in Figure 1 will always be parallel. Therefore, the polarization contribution to modulation a_P is unity for TE polarized interference. However, the interfering TM components (polarization in the plane of the page) will produce a modulation a_P that will fall off with the cosine of the angle β between the two TM components. TE polarized illumination will be utilized for this experiment in order to eliminate the reduction in modulation that is attributed to the TM component. The coherence contribution $\left|\gamma_{12}\right|$ is the dependence on the coherence of the illumination source and the relative phase variations between each interfering beam. The range of possible values for $\left|\gamma_{12}\right|$ is 0 to 1, where coherent illumination has a coherence term of unity, $\left|\gamma_{12}\right|$=1.

3. DEMODULATION THROUGH INTENSITY IMBALANCE

The aerial image that is created upon the interference of two mutually coherent beams may be demodulated by inducing an intensity imbalance between the two beams. If two interfering beams are assumed to have the same intensity, the aerial image distribution is given by:

$$I(x) = \frac{1}{2} + \frac{1}{2}\cos(Kx) \tag{3}$$

Where $K = 2\pi/\Lambda$ and Λ is the distribution period.[2] This relation is similar to the one developed earlier, however the maximum intensity has been normalized to unity and the phase relation has been expressed as a function of the spatial coordinate x. An intensity imbalance between the interfering beams may be generated by attenuating one of the beams during exposure, or alternatively by performing two independent exposures. In the first exposure, an aerial image intensity distribution with 100% modulation will be created by the two beams. The second exposure will demodulate this intensity distribution by blocking one of the beams completely and allow the unobstructed beam to deliver a DC intensity bias to the original aerial image. The demodulated intensity distribution assuming TE polarization and coherent illumination is given by:

$$I(x) = \frac{1}{2} + \frac{1}{2}a_I \cos(Kx) \tag{4}$$

where a_I is the induced level of modulation due to the intensity imbalance. The two pass exposure method of inducing demodulation that is described above may be mathematically visualized in terms of the delivered dose by adjusting the following intensity relation:

$$I = \underbrace{2I_1 \cdot (1+\cos\delta)}_{2-Beam} + \underbrace{I_2}_{\substack{Single \\ Beam}} \tag{5}$$

The 2-beam exposure and the single beam exposure can be derived by taking a product of equation (5) with the appropriate exposure times t_1 and t_2, respectively:

$$D = D_1 + D_2 = \underbrace{2I_1 \cdot t_1 \cdot (1+\cos\delta)}_{2-Beam} + \underbrace{I_2 \cdot t_2}_{\substack{Single \\ Beam}} \tag{6}$$

The result is the total dose D or total energy per incident area, where $D_n = I_n \cdot t_n$ and n is the exposure pass. The modulation (contrast) is found by taking the ratio of the difference to the sum of the maximum and minimum doses:

$$a_I = \frac{D_{\max} - D_{\min}}{D_{\max} + D_{\min}} = \frac{2I_1 \cdot t_1}{2I_1 \cdot t_1 + I_2 \cdot t_2} \tag{7}$$

If the demodulation is viewed as an imbalance over time rather than intensity then it may be assumed that $I_1 \approx I_2$ and t_2 is some percentage p of t_1, giving:

$$a_I = \frac{2}{2+p} \tag{8}$$

The modulation a_{DF} attained from defocusing a projection lithography system is equated to a_I in order to calculate the percentage p of time t_1 that a single beam exposure must be conducted, rather than a two-beam exposure.

4. MODULATION TRANSFER CURVES

The equivalent single beam second pass exposure required in a two-beam system, to synthesize the effects of defocus on a projection system, was theoretically determined by matching the aerial images for each defocus condition through the respective modulations. The PROLITH[3] lithography process optimization tool was used to facilitate the aerial image comparisons. Defocus conditions in a variety of optical configurations, including several different mask pitches and illumination schemes, were simulated and the resulting aerial image modulations were extracted. These modulations were fed into equation (8) in order to determine the necessary second pass exposure to achieve the same level of modulation in a two-beam interferometer. Coherent illumination and a chromeless phase-shift mask (CPSM) were used to generate the model for the interferometer. A pupil filter was used to block one of the diffraction orders to simulate a single second exposure pass. In order to quickly and efficiently determine the necessary single beam exposure to synthesize a particular defocus in a projection system a "Modulation Transfer Curve" may be mapped out as pictured in Figure 2. A modulation is determined from a specified defocus condition and then translated into the appropriate single beam exposure multiplier for two beam interference.

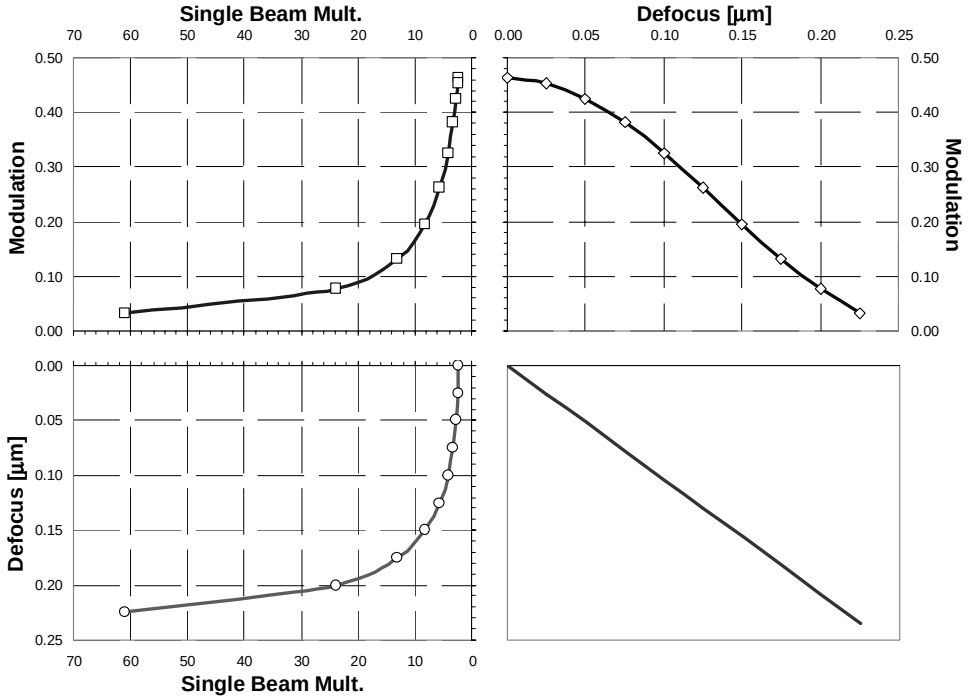

Figure 2. Modulation Transfer Curve for the synthesis of a partially coherent source configuration ($\sigma = 0.3$) and 1:1 89nm features at a k_1 of 0.35. Defocus was varied from 0 to 225nm.

5. IMPLEMENTATION OF SYNTHETIC DEFOCUS

A tabletop two-beam interference system was developed to demonstrate the ability of interferometric lithography to synthesize defocus in a projection system. The tabletop interferometric system is capable of conducting both dry and wet exposures. The optical setup for wet exposures is facilitated by the use of a fused silica half ball. The interferometer schematic is depicted in Figure 3. The illumination source for the set up was a 248nm KrF line narrowed excimer laser source, which was optimized by first passing it through a beam expander, a polarizer and a spatial filter before it entered

the interferometer. The bandwidth of the laser is line narrowed; using an unstable resonator, down to 10pm, and the spatial coherence is specified at 2mm.

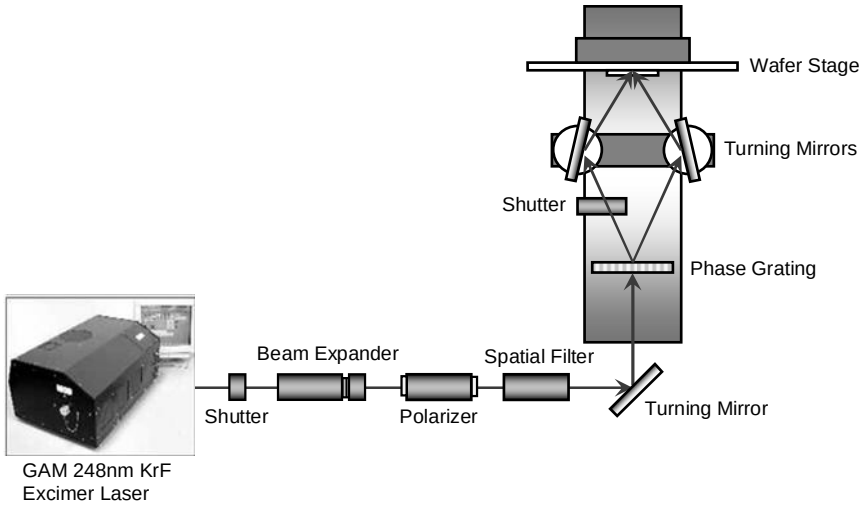

Figure 3. Table top lithography system for performing wet and dry interferometric exposures.

Spatial coherence is critical to affording the interference system a higher tolerance to misalignment. The source should be spatially coherent on the order of a few millimeters since the exposed field in this experiment was roughly 2-3mm in diameter. A 5x beam expander was utilized to expand the spatial coherence of the laser source. As a consequence of the beam expansion, the area over which the beam was spatially coherent was also magnified. The higher spatial coherence will provide better contrast when imaging, however one of the major disadvantages is that speckle may be evident in the final image. Speckle is the existence of ghost images and parasitic interference in the final resist image, which is generated from optics without antireflective coatings, as well as dust and debris on any optic surfaces. These conditions were averted by ensuring that all optical surfaces had an antireflective coating, in addition to regular optics cleaning.

As mentioned previously, TE polarization is preferred to TM since the modulation of TE polarized light is unity while the modulation of the TM state falls off as the cosine of the interference angle increases. A Rochon polarizer was used to separate the TE and TM polarization states. A Rochon polarizer separates the two polarization states through the use of two single crystal prisms, which are cut, polished and glued together with their optical axes orthogonal to one another. Due to the conflicting crystal orientations between each prism, a refractive index discontinuity is created at the interface of the two prisms. The optical axis of the first prism encountered by a beam of light is oriented perpendicular to the incident face of the prism. The polarization state of the beam that is oriented parallel to the optical axis of the second prism, or the ordinary ray, will see no change in refractive index and will continue on unaffected. However, the other polarization state, or extraordinary ray, will see the index discontinuity and diverge in accordance with the interface angle and the refractive index difference. The divergence of the two beams allows for the selection of TE over TM polarization by using an aperture.

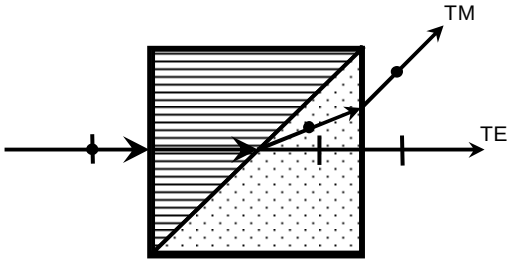

Figure 4. Configuration of the Rochon polarizer.

A spatial filter was introduced following the Rochon polarizer in order to "clean up" the beam due to a significant level of "ringing" and high frequency noise evident in the resist image. Ringing refers to noise or unwanted multiple-order energy peaks in an otherwise smooth Gaussian beam.[4] The noise in the beam profile was found to have been caused by a number of sources including dust in the air or on optical components, and Fresnel diffraction of the limiting aperture earlier in the system. The spatial filter removed most of the unwanted noise and passed only the primary diffraction order through the use of two pinholes and an excimer grade fuse silica spherical singlet lens. The spatial filter first reduces the TE output from the polarizer to a 1mm input beam diameter for the excimer grade singlet lens. The focal length of the singlet is approximately 152.1mm at a wavelength of 248nm, therefore the second pinhole is placed at that distance beyond the singlet to filter out any higher order noise. A clean Gaussian beam is then passed onto the turning mirror to be redirected into the interferometer whose edges were not interfered with throughout the remainder of the configuration, which avoided introducing any additional noise to the beam.

A 600nm pitch chromeless phase shifting diffraction grating was used to split the Gaussian beam so that the resulting $\pm 1^{st}$ diffraction orders may be interfered at the substrate surface.[5] This type of interferometer has been termed a "modified Talbot interferometer", however in this configuration turning mirrors have been added to allow for variable pitch. A phase shifting chromeless fused silica grating was used as a beam splitter because of its minimal complexity and preservation of beam energy once the beam was split. The diffraction angle of the 1st order beams is dependent on the pitch of the grating and the illumination wavelength, and is given by:

$$\theta_1 = \sin^{-1}\left(\frac{\lambda}{2 \cdot P_g}\right) \tag{9}$$

where P_g is the grating period and λ is the illumination wavelength. The $\pm 1^{st}$ diffraction orders generated by the phase shift mask are redirected by two turning mirrors and interfered at the image plane, whose rotation and vertical translation may also be adjusted. A variety of pitches are attainable by adjusting the height of the image plane and using the turning mirrors to redirect the beams so that they interfere at the new position of the image plane, as pictured in Figure 5.

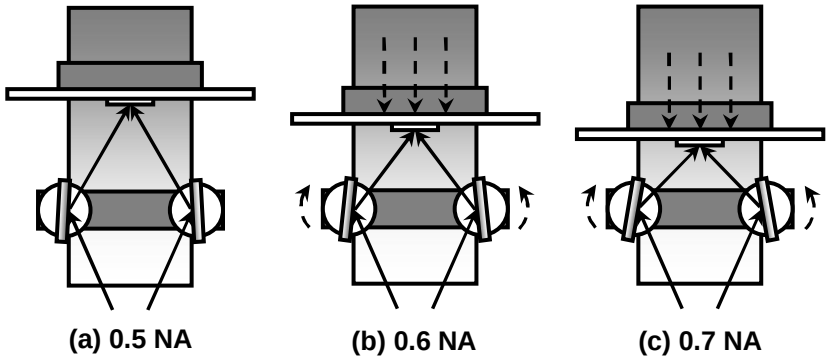

Figure 5. Pitch may be varied by adjusting the image plane and turning mirrors to the appropriate positions. NA's of (a) 0.5, (b) 0.6 and (c) 0.7 are pictured.

6. EXPERIMENTAL RESULTS

Exposures were carried out using an NA of 0.70, which yielded a pitch of 190nm for 248nm wavelength illumination. Modulations of 0.3, 0.5, 0.7 and 1.0 were implemented, by including a single beam exposure pass when conducting two-beam interference, for a time t_2 that was determined for each modulation using equation (8):

Modulation	Single beam multiplier
1.0	0.00
0.7	0.86
0.5	2.00
0.3	4.67

Table 1. Corresponding single beam multiplier for each modulation.

The single beam multipliers in Table 1 are used to calculate the exposure time necessary to induce the associated modulation by taking the product of this number with the two beam exposure time. The range of exposure times was independently calculated for the individual modulations by first finding the dose-to-clear and then estimating the exposure latitude that would provide a ±30% deviation, from the half-pitch, in CD. The chosen sample of CD's was presumed to be adequate for this analysis. The exposure increment was taken to be 2% of the dose-to-clear. The application of lower modulations would bring about a faster rate of variation in linewidth, therefore the exposure time range would be narrower and the sampling rate would be higher. This is desirable due to the difficult nature of printing lower modulations.

Top-down SEM images were taken for the modulation-exposure array. CD data was extracted for each field using the SuMMIT critical dimension analysis package.[6] The measured CD's were then used to estimate the induced modulation using the photoresist as a threshold detector. The CD data for each modulation was fit independently, using the threshold development model so that the dose-to-clear and modulation may be extracted.[2] The threshold development model is given by:

$$\frac{D}{D_S} = \frac{1}{1 + a_{meas} \cdot \cos\left(\pi \cdot CD \big/ \Lambda\right)} \tag{10}$$

where D is the exposure dose, D_S is the dose-to size, a_{meas} is the measured modulation and Λ is the printed pitch. The resulting measured modulation for the particular induced modulations are given in Table 2, as well as the exposure time to generate equal lines and spaces.

Induced modulation a_I	Measured modulation a_{meas}	Exposure time [sec] (equal *l:s*)
1.0	0.73	1.48
0.7	0.49	1.62
0.5	0.30	1.70
0.3	0.17	1.98

Table 2. Induced modulations with the extracted parameters a_I and the exposure time to generate equal lines and spaces.

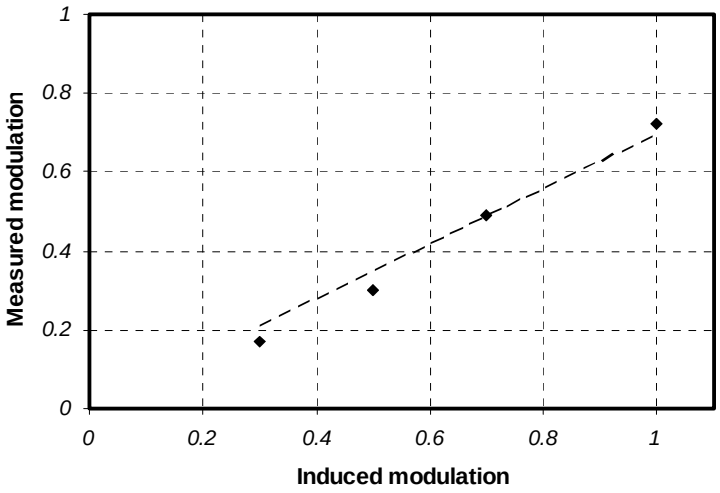

Figure 6. Linear fit extracted from the relation between the measured and induced modulations.

The extracted values of a_{meas} were plotted vs. a_I and a linear fit was applied to the data in order to estimate the intrinsic resist modulation, as shown in Figure 6. The intrinsic resist modulation was estimated to be 0.69. Despite limited data at lower modulations, due to poor exposure latitude and lack of quality images, the intrinsic modulation data followed well with the higher modulations. The data for the individual modulations is plotted in Figure 9 through Figure 12 in the appendix.

7. CONCLUSIONS

Interferometric lithography is capable of generating focus-exposure matrices to enable testing of new photoresist chemistries and developing RET's through the use of a synthetic focus generated by a second pass single beam exposure. The defocused aerial image of a specified projection system may be synthesized by applying the appropriate single beam exposure, which is determined by matching the aerial image modulation of the interferometric system with the projection system. The inexpensive nature and minimal complexity of this technique make it an attractive choice for the evaluation of emerging lithographic techniques, such as immersion, that would otherwise be cumbersome to reproduce experimentally.

8. APPENDIX

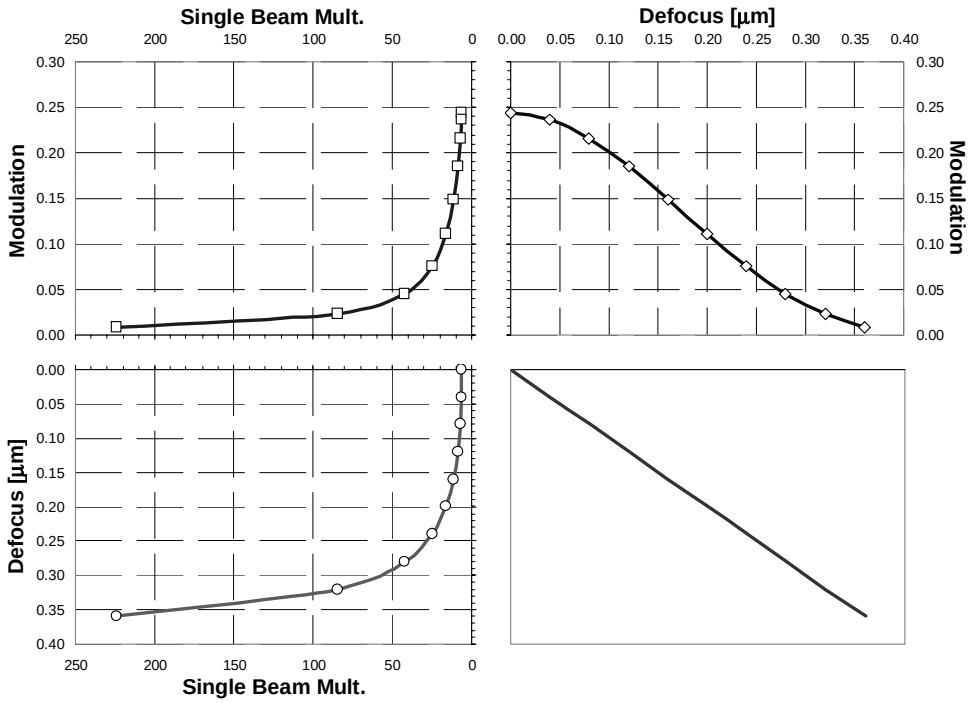

Figure 7. Modulation Transfer Curve for the synthesis of an annular source configuration (σ = *0.85/0.55*) and 1:1 89nm features at a k_1 of 0.35. Defocus was varied from 0 to 360nm.

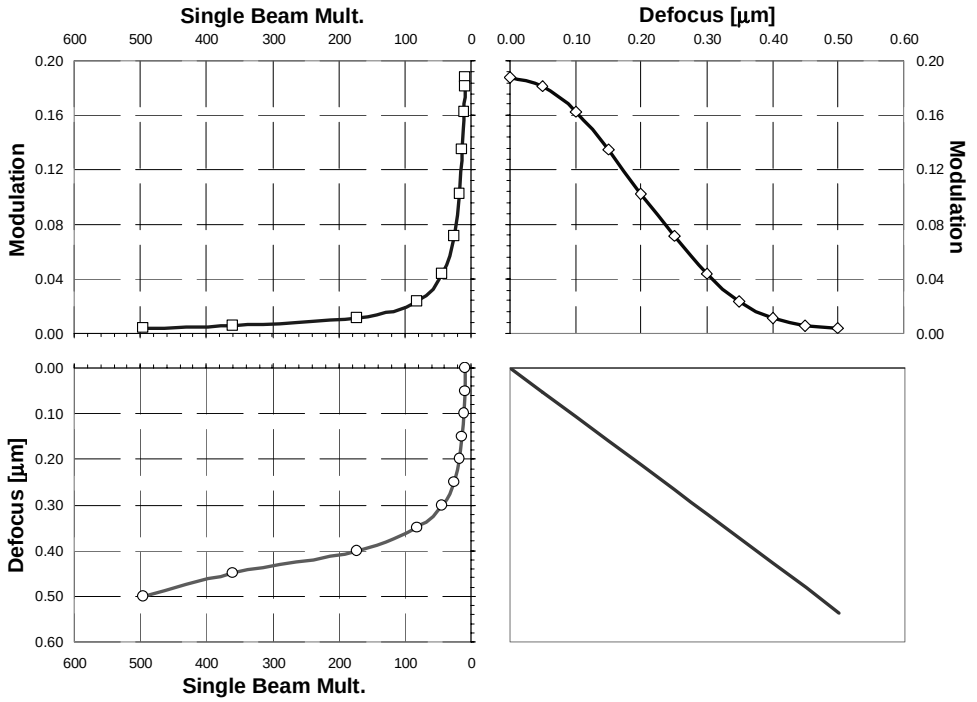

Figure 8. Modulation Transfer Curve for the synthesis of a quadrupole source configuration (σ = *0.85/0.20*) and 1:1 89nm features at a k_1 of 0.35. Defocus was varied from 0 to 500nm.

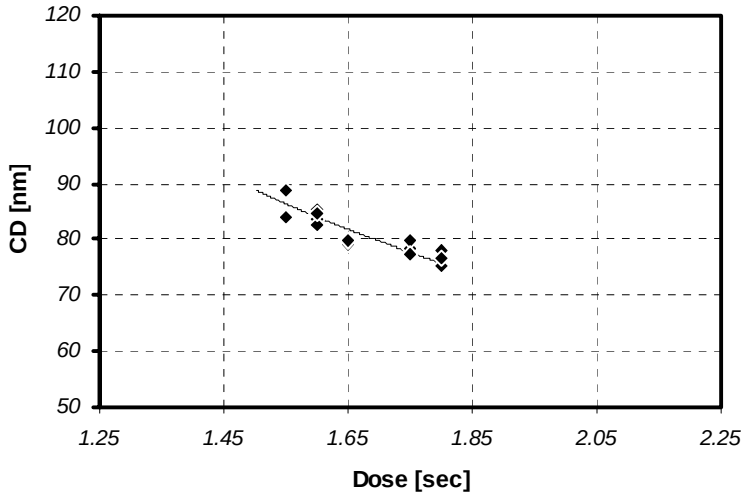

Figure 9. Dose vs. CD for $a_I = 1.0$; $a_{meas} = 0.73$.

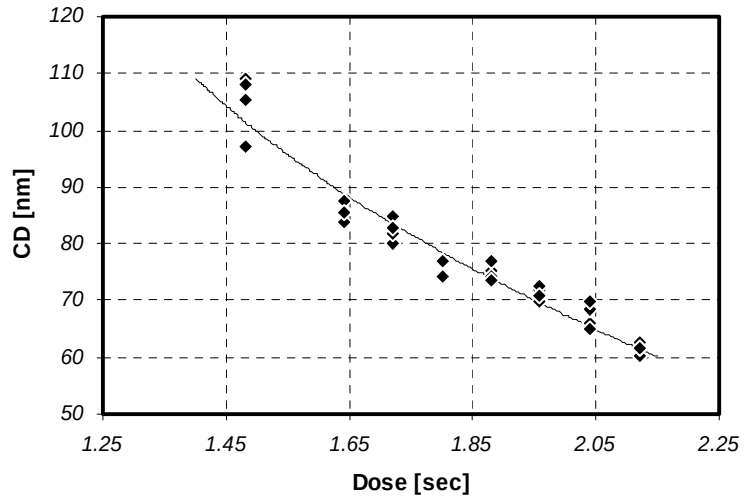

Figure 10. Dose vs. CD for $a_I = 0.7$; $a_{meas} = 0.49$.

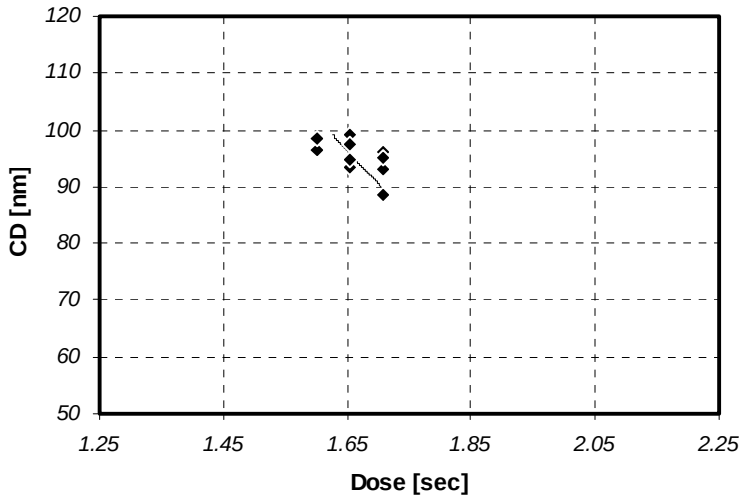

Figure 11. Dose vs. CD for $a_I = 0.5$; $a_{meas} = 0.30$.

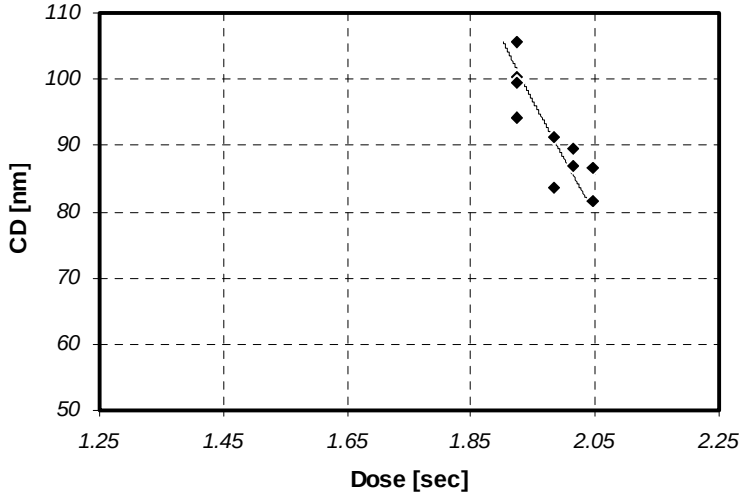

Figure 12. Dose vs. CD for $a_I = 0.3$; $a_{meas} = 0.17$.

9. REFERENCES

1 W. Hinsberg, F.A. Houle, J. Hoffnagle, M. Sanchez, G. Wallraff, M. Morrison, S. Frank, "Deep-ultraviolet interferometric lithography as a tool for assessment of chemically amplified photoresist performance", J. Vac. Sci. Technol., B 16 (6), 3689-3693, 1998

2 J.A. Hoffnagle, W.D. Hinsberg, M. Sanchez, F.A. Houle, M.I. Sanchez, "Characterization of photoresist spatial resolution by interferometric lithography", Proc. SPIE. Vol. 5038, 464-472 (2003)

3 PROLITH is a product of KLA-TENCOR – http://www.kla-tencor.com

4 A. Pete, "Understanding spatial filters", Edmunds Optics Technical Support, Edmunds Industrial Optics, Barrington, NJ 08007-1380

5 H. Kang, "New approaches in optical lithography technology for sub-79nm resolution, PhD Thesis, Rochester Institute of Technology (2004)

6 SuMMIT is a product of EUV Technology – www.euvl.com/summit/